

A MEASUREMENT OF THE SUNYAEV-ZEL'DOVICH EFFECT IN THE COMA CLUSTER OF GALAXIES

T. HERBIG,¹ C. R. LAWRENCE,² AND A. C. S. READHEAD

Owens Valley Radio Observatory, California Institute of Technology, Pasadena, CA 91125

AND

S. GULKIS

Jet Propulsion Laboratory, California Institute of Technology, Pasadena, CA 91109

Received 1994 July 25; Accepted 1995 June 1

ABSTRACT

We report the detection of the Sunyaev-Zel'dovich effect in the Coma cluster of galaxies with the 5.5 m telescope at the Owens Valley Radio Observatory. The measured decrement of the temperature of the cosmic microwave background is $\Delta T_{0,\text{obs}} = -270 \pm 29 \mu\text{K}$. After correcting for the effect of discrete radio sources and applying current models for the X-ray atmosphere of the cluster, we calculate the peak of the effect to be $\Delta T_0(0) = -505 \pm 92 \mu\text{K}$. Using the same X-ray models, and assuming spherical symmetry for the gas atmosphere, we derive a Hubble constant of $H_0 = 71_{-25}^{+30} \text{ km s}^{-1} \text{ Mpc}^{-1}$. This is the first detection of the Sunyaev-Zel'dovich effect in a nearby cluster of galaxies.

Subject headings: cosmic microwave background — distance scale — galaxies: clusters: individual (Coma)

1. INTRODUCTION

The Sunyaev-Zel'dovich effect (SZE) is the spectral distortion of the cosmic microwave background radiation (CMB) due to inverse Compton cooling of the X-ray gas in a cluster of galaxies (Sunyaev & Zel'dovich 1972). The change in the brightness temperature of the CMB is expressed as a function of observing frequency as

$$\frac{\Delta T}{T_{\text{CMB}}} = y \left(x \frac{e^x + 1}{e^x - 1} - 4 \right),$$

where $x = h\nu/kT_{\text{CMB}}$ and $y = (\sigma_T/m_e c^2) \int n_e kT_e dl$ is the Compton y -factor. In the Rayleigh-Jeans region, this leads to a temperature reduction of $\Delta T_0/T_{\text{CMB}} = -2y$.

In combination with X-ray observations, the SZE provides a powerful probe of the intracluster medium and can be used as a direct measurement of the Hubble constant (e.g., Silk & White 1978; Birkinshaw, Hughes, & Arnaud 1991). Since its first significant detection in 1984 (Birkinshaw, Gull, & Hardbeck 1984), the SZE has been measured with various techniques in several distant clusters of galaxies (Birkinshaw et al. 1991; Wilbanks et al. 1994; Jones et al. 1993) with redshifts ranging from 0.17 to 0.55 (Struble & Rood 1987; Dressler & Gunn 1992). However, more accurate astronomical and cosmological conclusions can be drawn from the SZE in nearby clusters, in which substantially better X-ray observations are possible. In the past, successful SZE detections in nearby clusters were precluded by the lack of sensitive instruments that could probe the large angular scales of these objects.

A prime candidate for such observations is the Coma cluster, Abell 1656 (Abell, Corwin, & Olowin 1989), at a redshift of 0.0235 (Sarazin, Rood, & Struble 1982). It is the richest nearby cluster free of strong radio sources, and has been studied extensively in all observational regimes. The cluster contains a large and hot X-ray atmosphere undisturbed

by a cooling flow (Watt et al. 1992). Even though it exhibits some amount of substructure (White, Briel, & Henry 1993), it is nevertheless a comparatively regular cluster with only slight apparent ellipticity.

During the winters of 1992 and 1993, we observed the Coma cluster with the recently completed 5.5 m radio telescope at the Owens Valley Radio Observatory (OVRO), a telescope dedicated to cosmic microwave background observations.

2. INSTRUMENT AND OBSERVING TECHNIQUE

Even clusters with very large and hot gas atmospheres only exhibit observable SZE temperature decrements of a few hundred microkelvin. Therefore, observations of the effect require a highly sensitive instrument with small and well-understood systematic errors.

The OVRO 5.5 m Cassegrain telescope has a receiver which operates at a center frequency of 32 GHz with a bandwidth of 5.7 GHz. The input of the cryogenic HEMT amplifier is switched every millisecond between two corrugated feeds that produce 7/3 beams separated by 22/2 on the sky in azimuth. The millisecond-sampling back end is fully digital to reduce potential systematic effects and to permit thorough testing of the entire system. To minimize the pickup of ground radiation, one of the most serious systematic effects, the telescope's secondary reflector is supported with a specially designed tripod structure (Lawrence, Herbig, & Readhead 1994).

During the 1992 season, the receiver noise temperature was 55 K; for the 1993 season an improved amplifier reduced this to 33 K. Further noise temperature contributions of 2 K from the CMB, 9 K from total ground pickup, and typically 8 K from the atmosphere produced total system temperatures of 74 K and 52 K for the two seasons, respectively.

Temperature calibration was performed several times during each observing season using hot and cold radiative loads, while the on-sky calibration is based on flux density measurements of DR 21, NGC 7027, 3C 286, Mars, and Jupiter (E. Leitch & A. Readhead 1995, private communication). This reveals a main beam efficiency of $70 \pm 4\%$, where the uncer-

¹ Hubble Fellow, Physics Department, Princeton University, Princeton, NJ 08544; herbig@puppp.princeton.edu.

² Postal address: Jet Propulsion Laboratory, California Institute of Technology, Pasadena, CA 91109.

tainty reflects both the internal consistency as well as the systematic errors from the absolute calibration of Cas A, Jupiter, and Mars. The corresponding aperture efficiency is $51\% \pm 3\%$. The resulting gain of 4.3 mK Jy^{-1} means that the telescope is not very sensitive to point sources, a distinct advantage in controlling the effects of discrete source contamination on our measurements. Gain calibration is accomplished every 15 minutes by comparison to an internal noise source. The telescope and its instrumentation tests are described in detail in Herbig (1994) and Herbig et al. (1995).

The $1/f$ knee of the total power channel is at approximately 2.5 Hz. To isolate the measurements from such low-frequency instabilities and to cancel offsets and linear drifts in the detected power, we follow a standard double differencing scheme (Readhead et al. 1989). At the first level, we Dicke switch between the two beams on the sky at 500 Hz, integrating $952 \mu\text{s}$ in each position. This is complemented by position switching every 20 to 30 s, producing flux measurement *points* with typical durations of 100 s. On the sky, they consist of the difference of a center beam and the average of two reference beams $22.2'$ away. Because all data are accumulated digitally, the reliability of each flux point can be estimated from the fluctuations of its constituent samples. Under pristine weather conditions, this internal error estimate corresponds to that expected from thermal fluctuations to within 10%. The beams are separated in azimuth; thus the reference beams sweep through arcs on the sky around the stationary center beam, traversing a range of parallactic angles ψ as the object is tracked across the sky.

Even though our double differencing technique reduces systematic effects by more than 5 orders of magnitude, the pickup of ground radiation still produces spurious signals from several tens to a few hundred microkelvins, depending on zenith angle. To eliminate this residual ground pickup, we are forced to introduce a third differencing step. We synchronously alternate between observations of the target field and a blank leading or trailing reference field at the same declination, but 15 minutes away in time (in 1992.0 coordinates). The telescope thus tracks the main and the reference fields over precisely the same path relative to the ground, producing a series of synchronized data “pairs” during each full cycle, ensuring that the subtraction of ground pickup is performed with strict overlap and with data taken in very similar atmospheric and ground conditions.

3. DATA

We observed three positions in the cluster: a central position (C), offset by a small distance ($3.5'$) to the southeast of the X-ray center (Abramopoulos et al. 1981) to minimize discrete source contamination; an off-center position $30'$ to the north of the cluster center (N); and another off-center position (CS) coincident with the south-western extension of the X-ray atmosphere (White et al. 1993), observed only in 1993. The coordinates of these positions are given in Table 1.

Atmospheric fluctuations affecting measurements with the 5.5 m telescope are much smaller at night than during the day. This implies that data should be taken from February until the end of the observing season in April, when Coma transits close to midnight. On the other hand, the weather in the Owens Valley during that period is generally worse than the very best weather during December and January. On balance, the

TABLE 1
OBSERVED VALUES

Position	$\alpha_{1950.0}$	$\delta_{1950.0}$	Season	$\Delta T_{0,\text{obs}}$	N_p
C	$12^{\text{h}} 57^{\text{m}} 30^{\text{s}}.0$	$+28^{\circ} 11' 00''$	1992	$-278 \pm 32 \mu\text{K}$	1588
			1993	-262 ± 50	1083
			overall	-270 ± 29	2671
N	$12^{\text{h}} 57^{\text{m}} 19^{\text{s}}.0$	$+28^{\circ} 43' 07''$	1992	-77 ± 60	620
			1993	-124 ± 70	321
			overall	-102 ± 44	941
CS	$12^{\text{h}} 54^{\text{m}} 31^{\text{s}}.0$	$+27^{\circ} 43' 40''$	1993	-9 ± 61	338

NOTES.—Microwave background decrements for each of the three observed positions, listed by observing season. The positions given are those of the center beam. $\Delta T_{0,\text{obs}}$ are the observed brightness temperatures on the sky, corrected for the frequency dependence of the SZE. These numbers are averages weighted by the internal error estimates of each data pair. The errors given are 1σ statistical uncertainties. N_p is the number of fully referenced data pairs used in the results. Roughly equal amounts of the usable data were obtained with the trailing and the leading reference fields.

day/night difference is more important, and we observed Coma only at night. Periods of bad weather were particularly frequent in 1993, when more than half of the continuously recorded data had to be rejected. Atmospheric conditions deteriorated in the spring, when positions N and CS were observed. Bad weather results in increased non-thermal fluctuations of the recorded signal, allowing us to exclude such periods during subsequent editing.

The full data set was edited in several ways. After applying the on-line calibration, we eliminated all data pairs in which the discrepancy in the positions with respect to the ground of the constituent data points exceeded $2'$ —this ensures proper ground subtraction, considering the beam size of $7.3'$. To identify data recorded during bad weather, we first discarded all individual data points whose internal scatter estimate exceeded the expected thermal noise by a factor of $f_n = 2$. To remove data affected by fluctuations on longer time scales, we identified all groups of such high-noise data and removed all preceding and subsequent neighbors within a margin equal to the duration of the rejected group (up to a maximum of 2 hr). This reduces our susceptibility to weather-induced biases not manifested by short-term fluctuations.

Finally, those data pairs whose values deviate by more than $f_o = 4\langle\sigma\rangle$ from the mean were removed iteratively while adjusting the mean to avoid “freezing in” an initial bias. This type of editing attempts to reduce the influence of non-Gaussian fluctuations in the data, where large deviations would be highly unlikely in a Gaussian distribution. This consideration motivates the value of f_o . Outlier editing affected 15 and 3 data pairs on positions C and N, respectively, while no outliers were present in the data on position CS. After the rejection of these outliers, the value for position C changed by $-22 \mu\text{K}$, and that for position N changed by $-16 \mu\text{K}$.

In all editing procedures, complete data pairs were removed to retain proper ground subtraction. Apart from outlier editing, no actual data values were used in the editing. The result is robust to different choices of the editing parameters. Once the internal noise cut is sufficient to excise the bulk of bad-weather data (at $f_n < 3$), the choice of f_n has no significant impact on the final result. In position C, 26% of all data pairs were removed by this criterion, while the margin criterion removed only another 5%. A further 28% of all data pairs

were removed in other editing steps, reflecting tracking problems that resulted in altaz overlap failure as well as other instrument problems. 59% of data pairs were retained for analysis. All data values were corrected for an atmospheric opacity of $\tau = 0.04$.

The edited results from the observations are given in Table 1, which shows Rayleigh-Jeans sky brightness temperatures corrected by 5.4% for the spectral dependence of the SZE. Apart from the subtractions inherent in our switching technique, no offsets or drifts were subtracted from the data. The overall result for the central position is a 9.3σ detection of the SZE; this result is highly significant even when split into individual observing seasons (see Table 1) or when split into subsets involving only leading or trailing reference fields. The cumulative results for positions N and CS are consistent with zero; their error bars are larger than those for position C due to shorter total integration times and worse atmospheric conditions.

The error bar for the 1992 data in position C is a factor of 2 larger than what is expected from thermal noise alone. We found that this degradation occurs on timescales from half an hour to several days, and suspect longer-term atmospheric fluctuations as its cause. From previous experience with single-dish CMB observations in the Owens Valley, such a degradation is not unexpected (Myers, Readhead, & Lawrence 1993). For the 1993 error this factor is 3.6, illustrating the worsened weather conditions during that season. However, systematic biases on the result produced by such long-term atmospheric conditions are reduced effectively by our triple subtraction technique. The errors in Table 1 are derived from the scatter of the sky signal only. Once the uncertainty in the calibration is applied as well, the overall observed value in position C becomes $\Delta T_{0,\text{obs}} = -270 \pm 33 \mu\text{K}$.

Figure 1 shows the data on position C binned as a function of parallactic angle ψ . Figure 1a shows the level of systematic effects, including ground pickup. Figure 1b demonstrates their cancellation using our synchronized referencing technique: the reduced χ^2 for the difference of these values from zero is 1.005 with 5 degrees of freedom. The fully referenced data are given in Figure 1c. The values at the extremes of the plot are well-determined because of longer integration times, and differ by $170 \pm 69 \mu\text{K}$. While large, this difference is not significant ($<2.5\sigma$) and cannot be taken as evidence for instrumental systematics (which would be unlikely because of the cancellation demonstrated in Figure 1b) or for real parallactic angle structure of the SZE.

4. DISCUSSION

The observed sky temperatures could be contaminated by discrete radio sources, reducing the observed SZE decrement if they affect the center beam. In principle, this can be corrected with high-resolution observations of the region at the same observing frequency. Owing to the large area of our telescope pattern on the sky, a list of discrete radio sources is difficult to identify at 32 GHz. However, a sample selected at a lower frequency can be substituted as long as it is sufficiently sensitive to identify all sources that could affect our result, depending on their spectra. A preliminary list of objects was identified from the 5C 4 and Condon surveys (Willson 1970; Becker, White, & Edwards 1991) and was observed with the OVRO 40 m telescope at 18.5 GHz to obtain spectral infor-

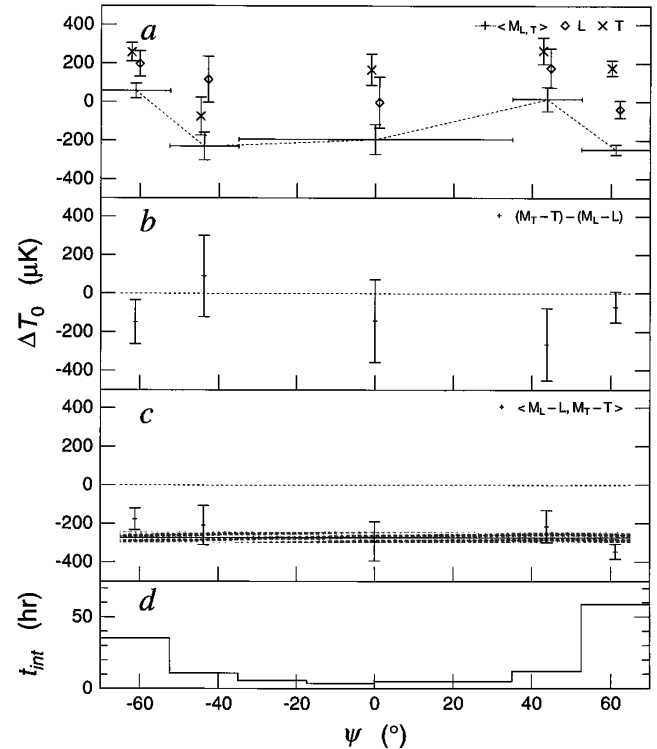


FIG. 1.—Microwave background measurements in the center of the Coma cluster (position C), binned by parallactic angle. The values shown are brightness temperatures on the sky, corrected for the frequency dependence of the SZE. (a) Double-switched data on the main field (M) and the leading (L) and trailing (T) reference fields separately, showing data contaminated by ground pickup. The reference fields lie consistently above the main field, which is shown as the average of data taken while synchronizing with the leading (M_L) and trailing (M_T) reference fields. The effective bin size is indicated by horizontal bars. (b) Difference between the referenced data on the leading and trailing reference fields; this difference cancels ground spillover and contains no sky signal. (c) Fully ground-subtracted data in position C—these data cancel ground spillover and contain the SZE in the Coma cluster. The average value of the SZE and its uncertainty is indicated by the horizontal line and the shaded region. (d) Total on-sky integration time within each bin (25% of which are spent on the center beam of the main field). The integration time is small in the central bins because Coma transits within 8° of the zenith at OVRO. For scheduling reasons, more time was spent at positive parallactic angles. The bin size of 17.5 represents independent patches on the sky. The four central bins were combined in panels (a)–(c) because of their short individual integration times.

mation. Only two of these sources contribute significantly to our data, and affect the center beam only: 5C 4.81 and 5C 4.85, to which we added Coma C (Venturi, Giovannini, & Feretti 1990), the cluster's central halo source. The correction for their influence is $-38 \pm 6 \mu\text{K}$. To account for sources with flat spectra ($\alpha > -0.5$, with $S_\nu \propto \nu^\alpha$), which may affect our measurement by more than $10 \mu\text{K}$ and yet fall below the flux density limits of those two lower-frequency surveys, an additional estimated allowance of $\pm 38 \mu\text{K}$ is made. A sensitive VLA survey is under way to eliminate this allowance. The source-corrected SZE decrement measured in position C thus becomes $\Delta T_{0,\text{sc}} = -308 \pm 51 \mu\text{K}$.

This result can be interpreted in the context of a combination of existing X-ray models (Hughes, Gorenstein, & Fabricant 1988; Briel, Henry, & Böhringer 1992) of the gas atmosphere. Under the assumption of spherical symmetry,

they describe the radial dependencies of electron density and temperature as

$$n_e(\theta) = n_e(0) \left[1 + \left(\frac{\theta}{\theta_c} \right)^2 \right]^{-3/2 \beta}$$

$$T_e(\theta) = \begin{cases} T_{\text{iso}} & \theta \leq \theta_{\text{iso}} \\ T_{\text{iso}} \left[\frac{1 + (\theta/\theta_c)^2}{1 + (\theta_{\text{iso}}/\theta_c)^2} \right]^{-3/2 \beta(\gamma-1)} & \theta > \theta_{\text{iso}} \end{cases}$$

The model parameters used here are listed in Table 2. Integrating the SZE produced by this model through the cluster and over the center and reference beams (which are not entirely outside the cluster), we predict that our observing configuration measures $\varepsilon_{\text{obs}}(\theta=0) = 61.0\% \pm 4.6\%$ of the central peak SZE at position C. This value contains the model dependence of the cluster atmosphere, with which we derive a maximum SZE decrement of $\Delta T_0(0) = \Delta T_{0,\text{sc}}/\varepsilon_{\text{obs}}(0) = -505 \pm 92 \mu\text{K}$ on a line of sight through the cluster center. The increased error bar reflects the uncertainty allowance of the discrete source subtraction and the quoted uncertainty of the X-ray model. For the same line of sight through the center of the cluster, the Compton spectral distortion is $y(0) = -\frac{1}{2} \Delta T_0(0)/T_{\text{CMB}} = 9.3 \pm 1.7 \times 10^{-5}$ and the Thomson optical depth is $\tau_T(0) = \sigma_T \int n_e dl = 5.6 \pm 1.1 \times 10^{-3}$.

The decrement $\Delta T_0(0)$ is derived with the assumption that the cluster has circular symmetry on the sky. If this should not be the case, then the observed decrement will depend on parallactic angle ψ , and a single value will not be sufficient to describe the cluster. As discussed above, our present data do not show statistically significant variations of the SZE with parallactic angle. However, this question can be settled only with a true image of the effect.

The Hubble constant can be derived because both the SZE and the X-ray surface brightness depend on the electron density. When the measured SZE is combined with the radial model of pressure and temperature from X-ray observations, n_e can be eliminated and the length along the line of sight through the cluster can be calculated. Assuming spherical symmetry and using the cluster's angular size, the absolute distance to the cluster can be calculated without recourse to any steps of the cosmic distance ladder. With our measurement and given the X-ray model described above, we find a Hubble constant of $H_0 = 71^{+30}_{-25} \text{ km s}^{-1} \text{ Mpc}^{-1}$. The error in this value reflects the statistical uncertainty of the SZE observations, the calibration of our system, the error in the corrections for known discrete radio sources, the allowance for as yet undetected discrete sources, and the quoted uncertainty of the X-ray model. However, it does not allow for the systematic error that originates from the choice of the X-ray model,

TABLE 2
X-RAY MODEL PARAMETERS

Parameter	Value	Reference
$n_e(0) \text{ (cm}^{-3}\text{)}$	$2.89 \pm 0.04 \times 10^{-3} h_{30}^{1/2}$	1
r_c	10.5 ± 0.6	1
β	0.75 ± 0.03	1
$T_{\text{iso}} \text{ (keV)}$	9.1 ± 0.4	2
r_{iso}	23^{+7}_{-5}	2

REFERENCES.—(1) Briel et al. 1992; (2) Hughes et al. 1988, assuming $\gamma = 1.555$. All errors are 1σ values.

possible departures from spherical symmetry, or clumping of the cluster gas (see, e.g., Birkinshaw et al. 1991).

Asphericity of the cluster along the line of sight cannot be ruled out, although our choice of the Coma cluster as the most nearby rich cluster does not expose us directly to this selection effect. The most effective remedy for this possibility is to observe a complete sample selected by total X-ray flux. Such observations are well under way at OVRO. Similarly, peculiar motion of the cluster with respect to the CMB can introduce a small additional Doppler-based SZE (Sunyaev & Zel'dovich 1980) of $\Delta T/T_{\text{CMB}} = -\tau_T v_{\text{pec}}/c$. Such peculiar motion has not been measured reliably enough to serve as a correction to our result. However, the effect would be small: a peculiar motion of $\pm 500 \text{ km s}^{-1}$ would affect our value of the Hubble constant by $\mp 4 \text{ km s}^{-1} \text{ Mpc}^{-1}$.

Given the dramatic progress in measurements of the SZE over the past few years, both with single dishes and with interferometers, the major uncertainty in their interpretation now lies in the choice of the X-ray model of the cluster atmosphere, which will be refined significantly by present and future observations with the *ROSAT* and *ASCA* telescopes.

This project would have been impossible without the dedication of H. Hardebeck, M. Hodges, and R. Keeney at the OVRO. Further thanks go to T. J. Pearson for his work on the telescope control system, to E. Leitch for his work on the telescope calibration, and to S. T. Myers, J. Baker, and M. Birkinshaw for many fruitful discussions. We appreciate the efforts of the National Radio Astronomy Observatory, TRW, and the Jet Propulsion Laboratory in designing and building the HEMT devices and amplifiers critical for this project. Microwave background studies at OVRO are supported under a grant from the National Science Foundation under grants AST91-19847 and AST94-19681. This work was also partially supported by NASA through Hubble Fellowship grant HF-1044.01-93A awarded by the Space Telescope Science Institute, which is operated by the Association of Universities for Research in Astronomy, Inc., for NASA under contract NAS 5-26555.

REFERENCES

- Abell, G. O., Corwin, H. G., & Olowin, R. P. 1989, *ApJS*, 70, 1
 Abramopoulos, F., Chanan, G. A., & Ku, W. H. M. 1981, *ApJ*, 248, 429
 Becker, R. H., White, R. L., & Edwards, A. L. 1991, *ApJS*, 75, 1
 Birkinshaw, M., Gull, S. F., & Hardebeck, H. 1984, *Nature*, 309, 34
 Birkinshaw, M., Hughes, J. P., & Arnaud, K. A. 1991, *ApJ*, 379, 466
 Briel, U. G., Henry, J. P., & Böhringer, H. 1992, *A&A*, 259, L31
 Dressler, A., & Gunn, J. E. 1992, *ApJS*, 78, 1
 Herbig, T. 1994, Ph.D. thesis, Caltech
 Herbig, T., Readhead, A. C. S., Lawrence, C. R., Pearson, T. J., Hodges, M. W., & Hardebeck, H. E. 1995, in preparation
 Hughes, J. P., Gorenstein, P., & Fabricant, D. 1988, *ApJ*, 329, 82
 Jones, M., Saunders, R., Alexander, P., Birkinshaw, M., & Dillon, N. 1993, *Nature*, 365, 320
 Lawrence, C. R., Herbig, T., & Readhead, A. C. S. 1994, *Proc. IEEE*, 82, 763
 Myers, S. T., Readhead, A. C. S., & Lawrence, C. R. 1993, *ApJ*, 405, 8
 Readhead, A. C. S., Lawrence, C. R., Myers, S. T., Sargent, W. L. W., Hardebeck, H. E., & Moffet, A. T. 1989, *ApJ*, 346, 566
 Sarazin, C. L., Rood, H. J., & Struble, M. F. 1982, *A&A*, 108, L7
 Silk, J., & White, S. D. M. 1978, *ApJ*, 226, L103
 Struble, M. F., & Rood, H. J. 1987, *ApJS*, 63, 543
 Sunyaev, R. A., & Zel'dovich, Y. B. 1972, *Comm. Astrophys. Space Sci.*, 4, 173
 ———, 1980, *MNRAS*, 190, 413
 Venturi, T., Giovannini, G., & Feretti, L. 1990, *AJ*, 99, 1381
 Watt, M. P., Ponman, T. J., Bertram, D., Eyles, C. J., Skinner, G. K., & Willmore, A. P. 1992, *MNRAS*, 258, 738
 White, S. D. M., Briel, U. G., & Henry, J. P. 1993, *MNRAS*, 261, L8
 Wilbanks, T. M., Ade, P. A. R., Fischer, M. L., Holzappel, W. L., & Lange, A. E. 1994, *ApJ*, 427, 75
 Willson, M. A. G. 1970, *MNRAS*, 151, 1